



Exotic vortex states in layered superconductors created by tilted magnetic field: Josephson vortices, solitons, vortex chains. . .

A.E. Koshelev

Materials Science Division, Argonne National Laboratory, 9700 South Cass Avenue, Argonne, IL 60439, USA

Abstract

In very anisotropic layered superconductors tilted magnetic field generates two interpenetrating vortex sublattices. This set of crossing lattices contains a sublattice of Josephson vortices (JVs) and a sublattice of pancake vortex (PV) stacks. The PV sublattice modifies structure of an isolated JV. The JV phase field is composed of the regular and vortex phases. The contribution from the vortex phase smoothly takes over with increase of the magnetic field. The core structure experiences qualitative evolution with anisotropy decrease. At large anisotropies JV weakly distorts PV crystal and the JV core contains many PV rows. At smaller anisotropies the JV core shrinks to one PV row and PV stacks in this central row form a soliton-like structure. At very small c -axis field ($\lesssim 1$ G) the PV stacks form chains located at JVs. At certain field the crossing-lattices chains transform into the tilted-vortices chains. We present a simple criterion for this transition.

© 2004 Elsevier B.V. All rights reserved.

PACS: 74.25.Qt

Keywords: Layered superconductors; Vortex lattices; Josephson vortices; Pancake vortices

1. Introduction

Vortex phase diagram of layered superconductors in tilted magnetic field is very rich and not completely understood. At very high anisotropies, γ , higher than the ratio of the London penetration depth λ to the interlayer spacing s , the ground state configuration in tilted field is given by crossing vortex lattices of the Josephson vortices (JVs) and stacks of pancake vortices (PVs) [2,3]. This situation is realized in the most anisotropic high- T_c compound $\text{Bi}_2\text{Sr}_2\text{CaCu}_2\text{O}_x$ (BSCCO).

In this proceeding we consider two very different regimes of the crossing vortex lattices. In the first part we study the structure of an isolated JV inside the dense PV lattice. We consider influence of the PV crystal on the JV core structure and distribution JV magnetic field (see also [9]). In the second part we consider the regime of a

very small concentration of PV stacks where they form a dilute array of chains located at JVs. We study the phase transition between the crossing-lattices chain and tilted-vortices chain, which was suggested in Ref. [6] to interpret experimental observations of Ref. [4].

2. Energy of vortex state

Structure of the vortex state in the layered superconductor is completely described by the PV coordinates in the layers $\mathbf{R}_{n,i}$, the regular phase $\phi_{rn}(\mathbf{r})$ and vector-potential $\mathbf{A}_r(\mathbf{r})$. The total phase and vector-potential can be split into the vortex and regular contributions, $\phi_n = \phi_{vn} + \phi_{rn}$ and $\mathbf{A} = \mathbf{A}_v + \mathbf{A}_r$. The vortex contributions minimize the energy for fixed PV positions for zero Josephson energy and give magnetic interaction energy for the PVs. In general, the regular contributions may include phases and vector potentials of the JVs. The total energy, $F[\phi_{rn}, \mathbf{A}_r, \mathbf{R}_{n,i}]$, naturally splits into the regular

E-mail address: koshelev@msd.anl.gov (A.E. Koshelev).

part $F_r[\phi_{rn}, \mathbf{A}_r]$, the PV magnetic interactions energy $F_M[\mathbf{R}_{n,i}]$, and the Josephson energy $F_J[\phi_{rn}, \mathbf{A}_r, \mathbf{R}_{n,i}]$, which couples the regular and vortex degrees of freedom,

$$F = F_r + F_M + F_J \quad (1)$$

with

$$F_r = \sum_n \int d^2\mathbf{r} \frac{J}{2} \left(\nabla \phi_{rn} - \frac{2\pi}{\Phi_0} \mathbf{A}_{r\perp} \right)^2 + \int d^3\mathbf{r} \frac{\mathbf{B}_r^2}{8\pi}, \quad (2)$$

$$F_M = \frac{1}{2} \sum_{n,m,i,j} U_M(\mathbf{R}_{n,i} - \mathbf{R}_{m,j}, n - m), \quad (3)$$

$$F_J = \sum_n \int d^2\mathbf{r} E_J \left(1 - \cos \left(\phi_{n+1} - \phi_n - \frac{2\pi s}{\Phi_0} A_z \right) \right), \quad (4)$$

where $J \equiv s\Phi_0^2[\pi(4\pi\lambda)^2] \equiv s\varepsilon_0/\pi$ is the phase stiffness, $E_J \equiv \Phi_0^2/[s\pi(4\pi\gamma\lambda)^2]$ is the Josephson coupling energy, and

$$U_M(\mathbf{R}, n) = \frac{J}{2\pi} \int \frac{\exp[i\mathbf{k}\mathbf{R} + iqn]}{k^2[1 + \lambda^{-2}(k^2 + 2(1 - \cos q)/s^2)^{-1}]} d\mathbf{k}dq$$

is the magnetic interaction between PVs [1].

3. Josephson vortices and solitons inside dense pancake lattice (see also [9])

3.1. High anisotropy: effective phase stiffness

In this section we consider the case of very high anisotropy $\gamma \gg \lambda/s$ when one can conveniently describe the JV structure in terms of the effective phase stiffness [3]. The approach is based on observation that a smooth transverse lattice deformations $\mathbf{u}_n(\mathbf{r})$ produce large-scale phase variations $\phi_{vn}(\mathbf{r})$ with $\nabla \phi_{vn} = 2\pi n_v \mathbf{e}_z \times \mathbf{u}_n$. At $B_z > \Phi_0/(\gamma s)^2$ the transverse elastic energy, F_{v-t} , can be rewritten in terms of $\phi_{vn}(\mathbf{r})$ as

$$F_{v-t} = \int \frac{d\mathbf{k}}{(2\pi)^3} \frac{J_v(B_z, \mathbf{k})}{2s} k_\perp^2 |\phi_v(\mathbf{k})|^2, \quad (5)$$

where the vortex phase stiffness $J_v(B_z, \mathbf{k})$ is related to the tilt and shear stiffness of the lattice [3]. In the range of wave vectors relevant for JV one can neglect the shear term and derive

$$J_v(B_z) \approx J \frac{B_\lambda}{B_z}, \quad B_\lambda \equiv \frac{\Phi_0}{4\pi\lambda^2} \ln \frac{r_{\text{cut}}}{r_w} \quad (6)$$

with $r_w \sim u_1(0)$ and $r_{\text{cut}} \sim \min(a, \lambda)$. The phase stiffness energy (5) has to be supplemented by the Josephson energy. In the core region we can neglect the vector-potentials and write the total energy in terms of ϕ_{rn} and ϕ_{vn} as

$$F = \sum_n \int d^2\mathbf{r} \left[\frac{J}{2} (\nabla \phi_{rn})^2 + \frac{J_v}{2} (\nabla \phi_{vn})^2 + E_J (1 - \cos(\phi_{n+1} - \phi_n)) \right]. \quad (7)$$

Excluding the regular phase, $\phi_{rn} = \phi_n - \phi_{vn}$, and varying the energy with respect to ϕ_{vn} at fixed ϕ_n , we obtain $\phi_{vn} = [J/(J_v + J)]\phi_n = [B_z/(B_z + B_\lambda)]\phi_n$. Substituting this relation in Eq. (7), we obtain the energy in terms of the total phase

$$F = \sum_n \int d^2\mathbf{r} \left[\frac{J_{\text{eff}}}{2} (\nabla \phi_n)^2 + E_J (1 - \cos(\phi_{n+1} - \phi_n)) \right], \quad (8)$$

which coincides with the phase energy at $B_z = 0$, except that the phase stiffness J is replaced by the effective phase stiffness J_{eff} ,

$$J_{\text{eff}}^{-1} = J^{-1} + J_v^{-1} \quad \text{or} \quad J_{\text{eff}} = J/(1 + B_z/B_\lambda). \quad (9)$$

Note that the smallest stiffness from J and J_v dominates in J_{eff} . For the Josephson vortex located between the layers 0 and 1 the phase satisfies the conditions $\phi_1 - \phi_0 \rightarrow 0$, for $y \rightarrow \infty$ and $\rightarrow 2\pi$, for $y \rightarrow -\infty$. Far away from the core the phase has the usual form for the vortex in anisotropic superconductor $\phi_n(y) \approx \arctan(\lambda_J(n - 1/2)/y)$, where the effective Josephson length

$$\lambda_J = \sqrt{J_{\text{eff}}/E_J} = \lambda_{J0}/\sqrt{1 + B_z/B_\lambda} \quad (10)$$

determines the core size, and $\lambda_{J0} = \gamma s$. Therefore, at low temperatures the JV core shrinks in the presence of PVs due to softening of the in-plane phase deformations. The JV energy per unit length, \mathcal{E}_{JV} , is given by $\mathcal{E}_{JV} = \pi\sqrt{E_J J_{\text{eff}}} \ln(L/s)$, where L is the cutoff length, which is determined by screening at large distances. At $B_z > B_\lambda$ the maximum PV displacement can be estimated as $u_{\text{max}}/a \approx 0.5\lambda/\lambda_{J0}$, which shows that the linear elasticity is applicable if $\gamma \gtrsim 3\lambda/s$. At $B_z > B_\lambda$ a number of PV rows within the JV core $N_{\text{rows}} \approx \lambda_{J0}/2\lambda$ is almost field independent.

The above description is valid only at $\gamma \gg \lambda/s$ and at low temperatures, when one can neglect fluctuation suppression of the Josephson energy. Thermal motion of the PVs at finite temperatures induces the fluctuating phase $\tilde{\phi}_{n,n+1}$ and suppresses the effective Josephson energy, $E_J \rightarrow CE_J$ where $C \equiv \langle \cos \tilde{\phi}_{n,n+1} \rangle$. This leads to reduction of the JV energy and thermal expansion of its core.

3.2. Moderate anisotropy: crossover between Josephson cores and soliton-like cores

The ‘‘effective phase stiffness’’ approximation is only valid if γ is significantly larger than λ/s . In this section we extend our analysis to the region $\gamma \sim \lambda/s$. We consider the JV structure at low temperatures and not very

small c -axis field, $B_z > \Phi_0/(\gamma s)^2$. The JV core structure is completely determined by the displacements of PV rows $u_{n,i}$ and phase distribution. We will operate with the phase perturbation $\phi_n(\mathbf{r})$ with respect to phase distribution of the ideal PV crystal. This phase depends on both in-plane coordinates, i.e., the problem is three-dimensional. We split this phase into the contribution, averaged over the JV direction (x -axis), $\phi_n(y)$, and the oscillating in the x direction contribution, $\tilde{\phi}_n(x, y)$. Pancake displacements induce jumps of the average phase at the coordinates of the vortex rows Y_i , $\phi_n(Y_i + 0) - \phi_n(Y_i - 0) = 2\pi u_{n,i}/a$, where a is the PV lattice spacing. The oscillating phase induced by the row displacements becomes negligible already at the neighboring row. This allows us to separate the local contribution to the Josephson energy, \mathcal{E}_{loc} , coming from $\tilde{\phi}_n(x, y)$ and reduce three-dimensional problem to the two-dimensional problem of finding the average phase and row displacements. The energy per unit length in terms of the regular phase, $\phi_{rn}(y)$, and the row displacements, $u_{n,i}$, can be written as

$$\begin{aligned} \mathcal{E}_J = & \sum_n \int dy \left[\frac{J}{2} \left(\frac{d\phi_{rn}}{dy} \right)^2 + E_J (1 - \cos(\phi_{n+1} - \phi_n)) \right] \\ & + \frac{1}{2} \sum_{n,m,i,j} U_{Mr}(u_{n,i} - u_{m,j}, Y_{i,j}, n - m) \\ & + \sum_{n,i} \mathcal{E}_{\text{loc}}(u_{n+1,i} - u_{n,i}, \phi_{n+1,i} - \phi_{n,i}), \end{aligned} \quad (11)$$

where

- (i) $\phi_n(y) \equiv \phi_{rn}(y) + \phi_{vn}(y; u_{n,i})$ is the total phase, the vortex phase is composed of jumps at the row positions Y_i , $\phi_{vn}(y; u_{n,i}) = -(2\pi/a) \sum_i u_{n,i} \Theta(Y_i - y)$, where $\Theta(y)$ is the step-function.
- (ii) $U_{Mr}(x_{n,i} - x_{m,j}, Y_{i,j}, n - m)$ is the magnetic interaction between the vortex rows separated by distance $Y_{i,j} = Y_i - Y_j = b(i - j)$, $U_{Mr}(u, y, n) \equiv \frac{1}{a} \sum_m [U_M(x_0 + u - ma, y, n) - U_M(x_0 - ma, y, n)]$ with $x_0 = 0$ or $a/2$.
- (iii) $\mathcal{E}_{\text{loc}}(u_{n+1,i} - u_{n,i}, \phi_{n+1,i} - \phi_{n,i})$ is the local Josephson energy due to the oscillating component of the phase difference, for $u \ll a$

$$\mathcal{E}_{\text{loc}}(u, \phi) \approx (\pi/2) E_J a \cos \phi (u/a)^2 \ln(0.39a/u).$$

We numerically minimized the energy with respect to row displacements and regular phase for different ratios $\alpha = \lambda/\gamma s$ and different B_z . We find that at small ratios, $\alpha < 0.3$, the core structure is consistent with the effective phase approach, i.e., PV displacements are small and the JV core includes many PV rows. With increase of this ratio, within the range $\alpha = 0.35\text{--}0.5$, the core structure experiences smooth yet qualitative evolution (see Fig. 1). For $\alpha = 0.5$ configuration of the PV rows in the central stack is very similar to the classical soliton (“kink”) of the stationary sine-Gordon equation: the stacks

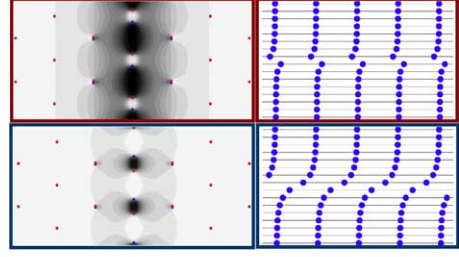


Fig. 1. Visualization of JV inside the PV lattice at $B_z = \Phi_0/(\gamma s)^2$. Left column represents $\cos(\phi_1 - \phi_0)$. Right column shows PV arrangements in the central row. Upper (lower) pictures represent the ratio $\lambda/\gamma s = 0.3$ (0.5) correspondingly.

smoothly transfer between the two ideal lattice position in the region of the core. One can estimate that the size of the soliton in z direction is given by λ/γ . Fig. 1 also shows the distribution of $\cos(\phi_1 - \phi_0)$. As one can see, at $\alpha = 0.3$ there are extended regions of large phase mismatch (dark regions), while for $\alpha = 0.5$ these regions are almost eliminated by large PV displacements in the core, so that the core region is essentially shrunked to a single row.

3.3. Large-scale behavior. Screening lengths

In this section we consider the JV structure at large distances from the core, $n \gg 1$, $y \gg \lambda_J$. At large distance screening of supercurrents becomes important and one can not neglect any more the vector potential. At these scales the phase changes slowly from layer to layer so that one can expand the Josephson energy in Eq. (4) with respect to phase difference and use continuous approximation. This reduces the Lawrence–Doniach model defined by Eqs. (1)–(4) to the anisotropic London model (see Ref. [5]). As this model is linear, it can be solved exactly by the Fourier transform, yielding the following results for the JV energy and magnetic field

$$\mathcal{E}_{\text{JV}} = \frac{J}{2s} \int \frac{d^2 \mathbf{k}}{\lambda^{-2} + \gamma^2 k_y^2 + k_z^2 (1 + w(\mathbf{k}))}, \quad (12)$$

$$B_x(\mathbf{k}) = \frac{\Phi_0}{1 + \lambda_c^2 k_y^2 + \lambda^2 k_z^2 (1 + w(\mathbf{k}))}, \quad (13)$$

where $w(\mathbf{k}) = 2h/[\lambda^2 k_y^2/2 + \ln(1 + k_z^2 r_{\text{cut}}^2)]$ is the PV renormalization factor and $h \equiv 4\pi n_s \lambda^2$. The integration has to be cut at $k_z \sim \pi/s$. In the limit $h \gg 1$ we estimate the JV energy and the magnetic field in the core as

$$\mathcal{E}_{\text{JV}} \approx \frac{2\pi J}{3\gamma s \sqrt{h}} \ln \left(\frac{0.2a}{r_w} \right)^{3/2},$$

$$B_x(0, 0) \approx \frac{\Phi_0}{3\pi \lambda \lambda_c \sqrt{h}} \left(\ln \frac{a}{r_w} \right)^{3/2}.$$

The magnetic field decays at the scale $\sim a/4.5$ in the z direction and at the scale $\gamma a^2/20\lambda$ in the y direction. The magnetic flux concentrated at this region is estimated as $\Phi \approx \Phi_0/(1 + 2.8h^2)$. The residual flux, $\Phi_0 - \Phi$, is distributed over the PV lattice at much larger distances.

4. Transition between crossing-lattices chains and tilted vortices chains at small fields

In this section we consider vortex states in very small c -axis field of the order of several gauss. It is known that at such small fields the PV stacks penetrate along the JVs forming isolated chains. Recently it was found that the PV stacks formed only when c -axis field exceed certain threshold value [4]. Later this observation have been interpreted as the first-order phase transition between the tilted-vortices chains at very small fields and the crossing-lattices chains at higher field [6]. Here we derive a simple analytical criterion for this transition.

We compare energies of two states: (i) the crossing-lattices chain with the spacing $c = Ns \ll \lambda$ between JVs and the spacing $a \gtrsim \lambda$ between PV stacks and (ii) tilted vortex chain with the tilt angle ϕ , $\tan \phi = a/c \ll \gamma$. The approximate energy of the dilute crossing-lattices chain per unit area, E_{CL} , is given by

$$E_{CL} \approx E_{PS}^s + \mathcal{E}_J + \frac{\epsilon_0}{\gamma c} (\ln N - 0.41) - \frac{\epsilon_x}{ac}$$

The first term is the energy of straight PV stacks, $E_{PS}^s \approx (\epsilon_0/a)(\ln(\lambda/\xi) + 0.5)$, the second term is the long-range Josephson energy, $\mathcal{E}_J = \pi\epsilon_0\lambda/(\gamma c^2)$, the third term is the local energy of the JVs, and the last term is correction from the crossing energy [3]. We neglected small contribution coming from the PV stack interactions. The energy of the tilted vortex chain at $\tan \phi \ll \gamma$ we evaluate as

$$E_{TV} \approx E_{PS}^s + \mathcal{E}_J + \frac{\epsilon_0}{a} \left(\frac{\pi\lambda}{a} + \ln \frac{a}{\lambda} - 1.72 + \frac{a^2(\ln N - 0.95)}{2(N\gamma s)^2} \right).$$

Comparing the above energies, we arrive at the transition criterion between the two states. Due to attractive coupling between the PV stacks [7], they should form clusters at small densities. However this does not influence much the location of the transition, because interaction between the stacks plays minor role. The boundary line is plotted in Fig. 2 for $\lambda/\gamma s = 0.4$. Elab-

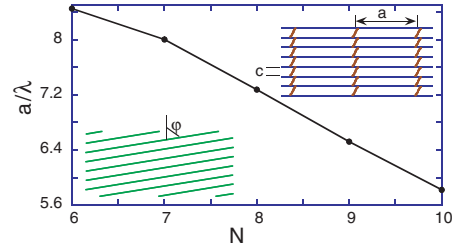


Fig. 2. Boundary separating the crossing-lattices chains and tilted-vortices chains for $\lambda/\gamma s = 0.4$.

orated numerical analysis shows that (i) at small fields a simple crossing configuration smoothly transfers into the strongly deformed intermediate configuration leading to significant downshift of the phase boundary shown in Fig. 2 and (ii) the first order transition transforms to crossover with increase of field. At fixed fields the transition can also be driven by the temperature, due to the T-dependence of λ , and the high-temperature phase corresponds to the tilted chains. This provides possible interpretation of disappearance of the field modulation in the chains with temperature increase observed in Ref. [8].

Acknowledgements

I would like to thank V. Vlasko-Vlasov, M. Dodgson, T. Tamegai, A. Grigorenko, and S. Bending for fruitful discussions. This work was supported by the U. S. DOE, Office of Science, under contract # W-31-109-ENG-38.

References

- [1] J.R. Clem, Phys. Rev. B 43 (1991) 7837.
- [2] L.N. Bulaevskii, M. Ledvij, V.G. Kogan, Phys. Rev. B 46 (1992) 366.
- [3] A.E. Koshelev, Phys. Rev. Lett. 83 (1999) 187.
- [4] A. Grigorenko et al., Nature 414 (2001) 728.
- [5] S.E. Savel'ev, J. Mirkovic, K. Kadowaki, Phys. Rev. B 64 (2001) 094521.
- [6] M.J.W. Dodgson, Phys. Rev. B 66 (2002) 014509.
- [7] A. Buzdin, I. Baladié, Phys. Rev. Lett. 88 (2002) 147002.
- [8] T. Matsuda et al., Science 294 (2001) 2136.
- [9] A.E. Koshelev, Phys. Rev. B 68 (2003) 094520.